EGR2 phosphatase regulates OST1 kinase activity and freezing tolerance in *Arabidopsis*

Yanglin Ding[1], Jian Lv[1], Yiting Shi[1], Junping Gao[2], Jian Hua[3] (ID), Chunpeng Song[4], Zhizhong Gong[1] & Shuhua Yang[1,*] (ID)

Abstract

OST1 (open stomata 1) protein kinase plays a central role in regulating freezing tolerance in *Arabidopsis*; however, the mechanism underlying cold activation of OST1 remains unknown. Here, we report that a plasma membrane-localized clade-E growth-regulating 2 (EGR2) phosphatase interacts with OST1 and inhibits OST1 activity under normal conditions. EGR2 is N-myristoylated by N-myristoyltransferase NMT1 at 22°C, which is important for its interaction with OST1. Moreover, myristoylation of EGR2 is required for its function in plant freezing tolerance. Under cold stress, the interaction of EGR2 and NMT1 is attenuated, leading to the suppression of EGR2 myristoylation in plants. Plant newly synthesized unmyristoylated EGR2 has decreased binding ability to OST1 and also interferes with the EGR2-OST1 interaction under cold stress. Consequently, the EGR2-mediated inhibition of OST1 activity is released. Consistently, mutations of *EGRs* cause plant tolerance to freezing, whereas overexpression of *EGR2* exhibits decreased freezing tolerance. This study thus unravels a molecular mechanism underlying cold activation of OST1 by membrane-localized EGR2 and suggests that a myristoyl switch on EGR2 helps plants to adapt to cold stress.

Introduction

Temperature is a key environmental cue along with sunlight and water that regulates plant growth and development. Extreme temperatures (high or low) adversely affect plant growth and survival, and these conditions are becoming more common due to climate change. Plants have evolved sophisticated mechanisms to respond and adapt to extreme temperatures (Guy, 1990). Cold acclimation is a process by which plants increase their tolerance to frost damage (< 0°C) after exposure to chilling temperatures (> 0°C; Guy, 1990; Thomashow, 1999). C-repeat (CRT)-binding factor (CBF)/dehydration-responsive element (DRE)-binding protein 1 (DREB1)-dependent signaling has extensive roles in cold acclimation (Stockinger *et al*, 1997; Liu *et al*, 1998; Thomashow, 1999). Cold stress rapidly induces the expression of *CBF* genes, and their encoding proteins directly activate a set of *cold-regulated* (*COR*) genes, leading to enhanced freezing tolerance (Stockinger *et al*, 1997; Liu *et al*, 1998; Thomashow, 1999). Cold-induced *CBF* expression is positively regulated by several transcription factors, including ICE1 (inducer of *CBF* expression 1), CAMTA3 (calmodulin-binding transcription activator 3), and BZR1 (brassinazole-resistant 1; Chinnusamy *et al*, 2003; Doherty *et al*, 2009; Li *et al*, 2017b). ICE1 functions as a master regulator of *CBF* expression (Chinnusamy *et al*, 2003). ICE1 is targeted for degradation after ubiquitination by HOS1 (high expression of osmotically responsive gene 1; Dong *et al*, 2006), whereas it is stabilized after sumoylation by SIZ1 (SAP and Miz; Miura *et al*, 2007). Recent studies showed that ICE1 protein is phosphorylated by protein kinases, including OST1 (open stomata 1) and MPK3/6 in *Arabidopsis*, and OsMAPK3 in rice (Ding *et al*, 2015; Li *et al*, 2017a; Zhang *et al*, 2017; Zhao *et al*, 2017; Shi *et al*, 2018). Under cold conditions, MPK3/6 phosphorylate ICE1 and promote ICE1 degradation in *Arabidopsis*, while OsMAPK3 phosphorylates and stabilizes OsICE1 in rice (Li *et al*, 2017a; Zhang *et al*, 2017; Zhao *et al*, 2017; Guo *et al*, 2018). Importantly, ICE1 is stabilized under cold stress after phosphorylation by cold-activated OST1, thereby promoting plant freezing tolerance (Ding *et al*, 2015). More recently, OST1 was found to interact with and phosphorylate BTF3 proteins, β-subunits of a nascent polypeptide-associated complex (NAC), and enhances their interaction with CBF proteins, thereby stabilizing CBF proteins under cold stress (Ding *et al*, 2018; Liu *et al*, 2018). Nevertheless, the molecular mechanism underlying cold activation of OST1 remains unclear.

Protein phosphatases that dephosphorylate phosphorylated proteins cooperate with sensor proteins to regulate stress responses in both eukaryotes and prokaryotes (Fuchs *et al*, 2013). Type 2C protein phosphatases (PP2Cs) are Ser-Thr protein phosphatases and

---

1 State Key Laboratory of Plant Physiology and Biochemistry, College of Biological Sciences, China Agricultural University, Beijing, China
2 College of Horticulture, China Agricultural University, Beijing, China
3 Department of Plant Biology, Cornell University, Ithaca, NY, USA
4 Institute of Plant Stress Biology, Collaborative Innovation Center of Crop Stress Biology, Henan University, Kaifeng, China
   *Corresponding author. Tel: +86 10 62734838; E-mail: yangshuhua@cau.edu.cn

are the largest protein phosphatase family in plants. In *Bacillus subtilis*, energy and nutritional deficiency responses are controlled by the energy sensor RsbQ together with the PP2C RsbP (Martinez *et al*, 2010). In *Arabidopsis thaliana*, ABA signaling is negatively regulated by the ABA receptors PYR/PYL/RCAR interacting with PP2Cs of clade A, such as ABI1 and ABI2 (Ma *et al*, 2009; Park *et al*, 2009; Yin *et al*, 2009). In *B. subtilis*, cold signals are perceived by plasma membrane-localized histidine kinase DesK, which has a dual role as protein kinase and protein phosphatase (Aguilar *et al*, 2001; Albanesi *et al*, 2004, 2009). Under normal temperatures, DesK acts as a phosphatase that removes the phosphoryl group from DesR. Cold temperatures induce conformational changes in the DesK tertiary structure that stimulate its histidine kinase activity, resulting in phosphorylation of the downstream regulator DesR, activation of the target gene *Des*, and maintenance of membrane fluidity (Albanesi *et al*, 2009; Cybulski *et al*, 2015). There is no evidence for a protein with both kinase and phosphatase activities under different stress conditions in plants, so it is possible that phosphatase (s) might cooperatively function with protein kinase(s) for cold signal sensing and signaling.

In this study, we identified a plasma membrane-localized clade-E growth-regulating 2 (EGR2) phosphatase as a negative regulator of plant freezing tolerance by inhibiting OST1 kinase activity. At normal temperature, EGR2 is associated with and myristoylated at the N-terminus by N-myristoyltransferase NMT1, which is important for EGR2 to interact with and inhibit OST1. Cold stress induces the accumulation of newly synthesized unmyristoylated EGR2 by compromising the EGR2-NMT1 interaction, leading to the decreased interaction of EGR2 and OST1, which consequently activates OST1 under cold stress. These results provide novel insights into the mechanism of cold activation of OST1 by membrane-localized EGR2.

Results

Cold-induced OST1 activity is independent of ABA receptors

We previously reported that OST1 protein kinase, a core component in ABA signaling, is activated by cold and positively regulate plant freezing tolerance (Ding *et al*, 2015). However, the mechanism underlying cold-mediated OST1 activation is hitherto unknown. It has been reported that the PYR/PYL (pyrabactin resistance/pyrabactin resistance like) ABA receptors are prominent regulators of OST1 activation in ABA signaling (Ma *et al*, 2009; Park *et al*, 2009). This prompted us to investigate whether ABA receptors are involved in cold-mediated OST1 activation by performing in-gel kinase assays using total proteins of wild-type plants and ABA receptor mutants. OST1 kinase activity was induced within 30 min of cold treatment and peaked after 2 h in wild-type plants (Figs 1A and B, and EV1A). These results are consistent with our previous results using *OST1*-overexpressing transgenic plants and *Arabidopsis* protoplasts (Ding *et al*, 2015). Moreover, we observed that OST1 was obviously activated by cold stress in ABA receptor mutants, including *pyr1 pyl1,4*, *pyr1 pyl1,2,4*, *pyr1 pyl4,5,8*, and *pyr1 pyl1,4,5,8* (Figs 1A and B, and EV1A). As a control, ABA-induced OST1 activity was drastically decreased in the *pyr1 pyl1,4* triple mutant after ABA treatment

(Fig EV1B), in agreement with previous reports (Ma *et al*, 2009; Park *et al*, 2009). These combined results suggest that cold activation of OST1 is independent of ABA receptors. Considering that OST1 kinase activity was significantly activated at 2 h after cold treatment, we selected 2 h as a time point for further studies.

Next, we determined OST1 kinase activity in *ABI1*-overexpressing (*ABI1-OE14*) transgenic plants (Ding *et al*, 2015), and *abi1 abi2 hab1* triple mutant after cold treatment using in-gel kinase assay. The OST1 kinase activity was decreased approximately 30% in *ABI1-OE14*, whereas enhanced twofold in *abi1 abi2 hab1* triple mutant (Fig 1C and D), suggesting that clade-A PP2Cs contribute to inhibiting OST1 kinase activity in response to cold stress, which is consistent with our previous study (Ding *et al*, 2015). However, it is worthy to note that OST1 kinase activity was not fully inhibited in *ABI1*-overexpressing plants (Fig 1C and D), implying that unknown protein phosphatase(s) might be also responsible for modulating cold-mediated OST1 activity.

EGR protein phosphatases interact with OST1

To identify protein phosphatases modulating OST1 activity under cold stress, we analyzed RNA-Seq data from our previous study (Jia *et al*, 2016). Nine genes encoding PP2C-type phosphatases were up- or down-regulated by cold treatment (Appendix Fig S1A).

Yeast two-hybrid analyses were performed to test whether these phosphatases interacted with OST1 and EGR2 (clade-E growth-regulating 2; At5g27930) was found to be an OST1-interacting protein (Fig 2A). *In vitro* pull-down assays showed that MBP-His-EGR2, but not MBP-His, interacted with GST-OST1 (Fig 2B). The interaction of OST1 and EGR2 was further verified *in N. benthamiana* leaves by co-immunoprecipitation (co-IP) assay (Fig 2C). EGR2 protein was previously shown to be localized at the plasma membrane (Bhaskara *et al*, 2017). We performed bimolecular fluorescence complementation (BiFC) assay and found that the interaction between OST1 and EGR2 occurred at the plasma membrane in protoplast cells (Fig 2D). In addition, we created *Super:EGR2-Myc* construct and generated *EGR2-Myc*-overexpressing transgenic plants. Mass spectrometry analysis with these transgenic plants identified OST1 as an EGR2-interacting partner (Appendix Table S1), further supporting that EGR2 interacts with OST1 *in planta*.

EGR2 was reported as a negative regulator of plant growth during drought stress, and it has two close homologs, EGR1 (At3g05640) and EGR3 (At3g16800; Bhaskara *et al*, 2017). We found that the expression of *EGR1* and *EGR3*, like *EGR2*, was up-regulated by cold stress (Appendix Fig S1B). Furthermore, EGR1 and EGR3 also interacted with OST1 *in vivo* (Appendix Fig S1C and D).

EGRs inhibit OST1 kinase activity

We next examined whether EGR2 was involved in regulating OST1 activity using *in vitro* phosphorylation assay. OST1 has auto-phosphorylation activity and phosphorylates its substrate ABF2 protein (Fig 2E). Interestingly, the auto-phosphorylation and kinase activities of OST1 were largely abolished when it was incubated with EGR2 (Fig 2E). A previous study showed that a conserved amino acid Gly180 of ABI1 or Gly168 of ABI2 located closely to Mg^{2+} coordination center that is important for their phosphatase activity (Vlad *et al*, 2009). This Gly was found in a conserved motif "DGHG*" in
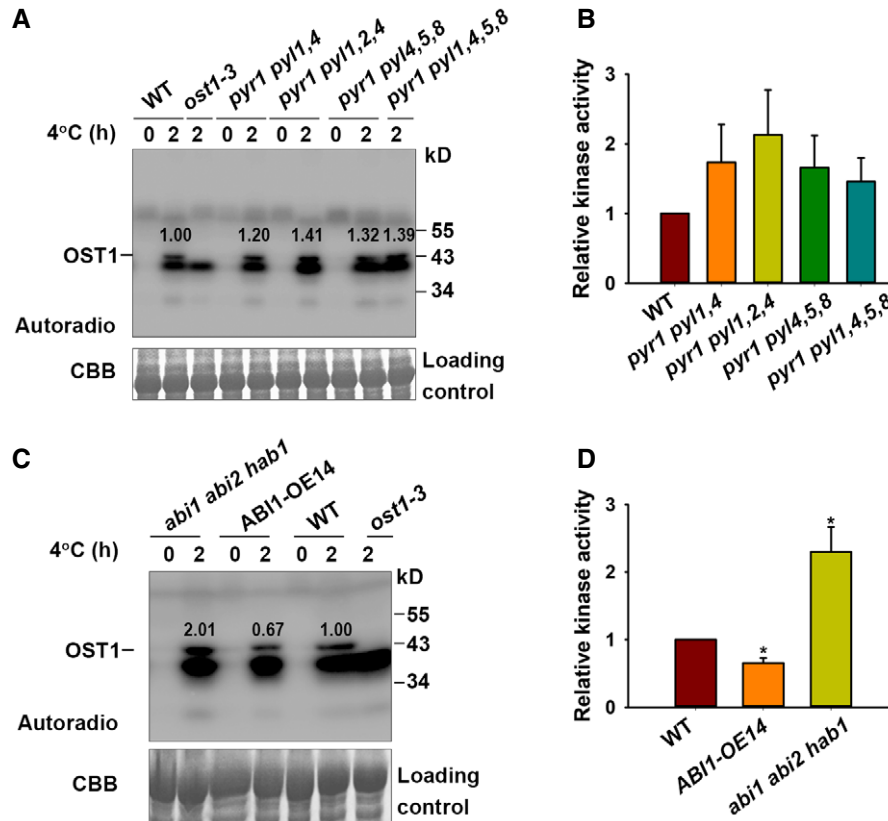
Figure 1. Cold-induced OST1 kinase activity is independent of ABA and ABA receptors.

A, B In-gel kinase assay of OST1 activity in ABA receptor mutants under cold stress. Ten-day-old wild-type, *ost1-3*, *pyr1 pyl1,4*, *pyr1 pyl1,2,4*, *pyr1 pyl4,5,8* and *pyr1 pyl1,4,5,8* mutants were treated at 4°C for 2 h. Total protein extracts were prepared and separated on SDS–PAGE gel containing 0.1 mg/ml GST-ΔABF2 as a substrate, and incubated with 60 μCi of [γ-^{32}P]ATP. Representative pictures are shown in (A), and relative kinase activity is shown in (B).

C, D In-gel kinase assay of OST1 activity in *ABI1-OE14* and *abi1 abi2hab1* mutants under cold stress. Representative pictures are shown in (C), and relative kinase activity is shown in (D).

Data information: In (A and C), Top, gel autoradiograph; bottom, Coomassie Brilliant Blue (CBB) staining of RuBisCO large subunit was used as a loading control. The ratio of band intensity of OST1 to RuBisCO in the wild type with cold treatment for 2 h was set to 1.00. In (B and D), each bar represents the mean ± SEM of three biological repeats. *$P < 0.05$ (two-tailed t-test).
Source data are available online for this figure.

type 2C phosphatases in *Arabidopsis* and other plant species (Robert *et al*, 2006). We analyzed EGR2 amino acid sequence and found the conserved Gly100 in EGR2 which might be involved in its dephosphorylation activity. We therefore mutated Gly100 to Asp100 (EGR2^{G100D}) to mimic its inactive form and performed *in vitro* phosphorylation assay. As expected, EGR2^{G100D} failed to repress OST1 auto-phosphorylation or kinase activity (Fig 2E). These results indicate that EGR2 dephosphorylates OST1 and thus represses OST1 kinase activity *in vitro*.

A previous study showed that PYL4 inhibits activities of clade-A PP2C phosphatases in ABA-dependent and ABA-independent manners (Hao *et al*, 2011). Therefore, we examined whether the phosphatase activity of clade-E phosphatase EGR2 was also regulated by ABA-PYL4 in an *in vitro* phosphorylation assay. Consistent with the previous study (Hao *et al*, 2011), ABA-PYL4 repressed ABI1-mediated OST1 dephosphorylation *in vitro* (Fig EV2A). However, ABA-PYL4 could not repress EGR2-mediated dephosphorylation of OST1 (Fig EV2B). These results suggest that

EGR2-mediated inhibition of OST1 activity is independent of the ABA receptor PYL4.

To determine whether OST1 activity was regulated by EGRs *in planta*, we obtained *egr1-1*, *egr1-2*, *egr2-1*, *egr2-3*, *egr3-1*, and *egr3-2* single mutants and subsequently generated the *egr1-2 egr2-3* (*egr1 egr2*) double mutant. Semi-qPCR analysis showed that *egr1-1* was a knockdown mutant, whereas the others were knockout mutants (Appendix Fig S2A and B). Next, we performed in-gel kinase assays using total proteins prepared from wild-type, *egr1*, *egr2*, and *egr3* single mutants, and *egr1 egr2* double mutant subjected to 4°C treatment for 2 h. The OST1 activity was consistently enhanced in *egr1*, *egr2*, and *egr3* single mutants compared with the wild-type plants under cold stress (Figs 2G and H, and Appendix Fig S2C and D). Strikingly, cold-induced OST1 activity was much higher in the *egr1 egr2* double mutant than in the single mutants (Fig 2F and G), suggesting that EGR1 and EGR2 function redundantly in regulating OST1 activity. We also examined the OST1 activity in *EGR2*-overexpressing transgenic plants (Appendix Fig S2E) and observed that
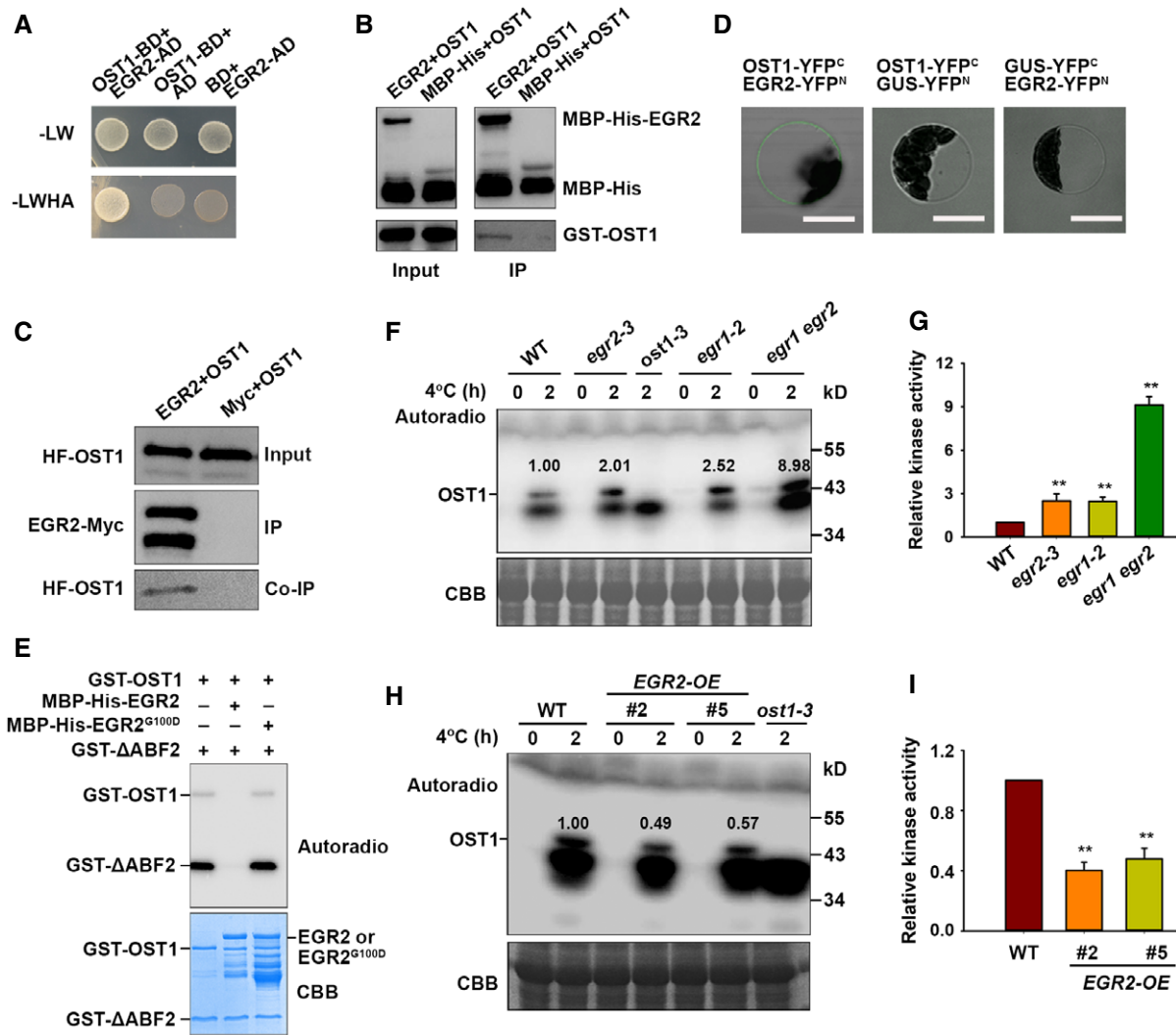
Figure 2. OST1 interacts with EGR2 and inhibits OST1 activity under cold stress.

A Interaction of OST1 and EGR2 in yeast. Yeast cells harboring different vector combinations were grown on SC/−Leu/−Trp medium for 3 days or SC/−Leu/−Trp/−His/−Ade medium for 6 days. OST1-BD/AD and BD/EGR2-AD were used as negative controls.

B OST1 interacts with EGR2 *in vitro*. Purified recombinant MBP-His-EGR2 or MBP-His proteins from *E. coli* were immunoprecipitated with MBP beads and then incubated with purified recombinant GST-OST1. Precipitated proteins were detected with anti-His and anti-GST antibodies.

C Co-IP assay of OST1 with EGR2 *in vivo*. *35S:HF-OST1/Super:EGR2-Myc* or *35S:HF-OST1/Super:Myc* was expressed in *N. benthamiana* leaves. Total proteins were immunoprecipitated with anti-Myc agarose beads, and the co-immunoprecipitation products were subjected to immunoblot analysis. EGR2-Myc and HF-OST1 were detected with anti-Myc and anti-HA antibodies, respectively.

D Bimolecular fluorescence complementation (BiFC) assay. Wild-type *Arabidopsis* protoplasts transformed with *OST1-YFP^C* and *EGR2-YFP^N* were incubated for 18 h. The interaction signal was detected by confocal microscopy. The combinations of OST1-YFP^C/GUS-YFP^N and GUS-YFP^C/EGR2-YFP^N were used as negative controls. Scale bars: 100 μm.

E EGR2 inhibits OST1 kinase activity *in vitro*. Proteins were incubated with 1 μCi [γ-^{32}P]ATP in kinase reaction buffer for 30 min at 30°C and then separated by SDS–PAGE. Top, autoradiograph; bottom, CBB staining.

F, G In-gel assay of OST1 activity in 10-day-old wild-type, *egr1* and *egr2* single mutants, and the *egr1 egr2* double mutant under cold stress.

H, I In-gel assay of OST1 activity in 10-day-old wild-type and *EGR2*-overexpressing plants under cold stress.

Data information: In (F–H), the ratio of band intensity of OST1 to RuBisCO in the wild type with cold treatment for 2 h was set to 1.00. In (F and H), representative pictures are shown: Top, autoradiograph; bottom, CBB staining. In (G and I), relative kinase activity is shown. Each bar represents the mean ± SEM of three biological repeats. **$P < 0.01$ (two-tailed *t*-test).

Source data are available online for this figure.

cold-induced OST1 activity was obviously decreased compared to the wild type (Fig 2H and I). These results suggest that EGRs negatively regulate OST1 activity under cold stress.

SnRK2.2 and SnRK2.3 are homologs of OST1 (Fujii *et al*, 2011). Thus, we tested whether EGR2 interacted with SnRK2.2 and SnRK2.3 and inhibited their kinase activity. We found that EGR2

also interacted with SnRK2.2 and SnRK2.3 proteins (Appendix Fig S2F and G). *In vitro* kinase assay proved that SnRK2.2 or SnRK2.3 kinase activity was also inhibited by EGR2 (Appendix Fig S2H).

OST1 was reported to stabilize ICE1 by phosphorylating ICE1 under cold conditions (Ding *et al*, 2015), which tempts us to ask whether ICE1 stability was affected by EGR2. HF-ICE1 proteins were expressed in wild-type, *egr2-3*, and *egr2-3 egr1-2* protoplasts and treated with or without 4°C for 3 h. We found that ICE1 protein was much more stable in the *egr2-3* and *egr1 egr2* mutants than that in the wild type after cold treatment (Appendix Fig S3A–D). Therefore, EGR1/2 promotes ICE1 degradation by repressing OST1 activity under cold stress.

Next, we dissected whether EGR2 affected the subcellular localization of OST1. Cell fractionation assays were performed, and the results showed that OST1 was localized at the cytosol and nucleus at both 22 and 4°C in wild-type and *egr2-3* mutant plant (Appendix Fig S4A and B). Interestingly, we found that a very little amount of OST1 protein was localized at the plasma membrane in wild-type and *egr2-3* plants (Appendix Fig S4C and D). Because no transmembrane domain was found in OST1, it is possible that OST1 is bound to the PM by binding with PM-localized proteins, including SLAC1, KAT1, RbohF (Geiger *et al*, 2009; Sato *et al*, 2009; Sirichandra *et al*, 2009), and EGR2. These combined results suggest that the activity of OST1 around PM is inhibited by EGR2 under normal temperature.

EGRs negatively regulate plant freezing tolerance

We next assessed whether EGRs were involved in regulating plant freezing tolerance. Under non-acclimated (NA) and cold-acclimated (CA) conditions, the *egr2-1* and *egr2-3* mutants displayed enhanced freezing tolerance with higher survival rates than the wild-type plants (Figs 3A and B, and EV3A and B). Ion leakage, an indicator of stress-induced PM injury, was dramatically lower in *egr2* mutants than in wild-type plants after freezing treatment (Figs 3C and EV3C). The freezing tolerance of *egr2-3* was fully complemented by *Myc*-tagged *EGR2* genomic fragments driven by the native promoter (*EGR2:EGR2-Myc*; Figs 3A–C, and EV3D and E). In addition, the *egr1-1*, *egr1-2*, *egr3-1*, and *egr3-2* mutants also displayed increased freezing tolerance compared with the wild type (Appendix Fig S5A–L). We also analyzed the freezing phenotypes of *egr1 egr2* double mutants and found that *egr1 egr2* double-mutant plants showed much more freezing tolerance than *egr1-2* and *egr2-3* single mutants under NA and CA conditions, indicating that EGR2 and EGR1 function redundantly in regulating plant freezing tolerance (Fig EV3F–H). Next, we analyzed the freezing tolerance of *EGR2*-overexpressing transgenic plants, which had lower freezing tolerance than the wild type with or without cold acclimation (Fig 3D). The survival rates of these transgenic plants were lower, whereas ion leakage was higher than the wild type after freezing treatment (Fig 3E and F). These results indicate that EGRs negatively regulate plant freezing tolerance.
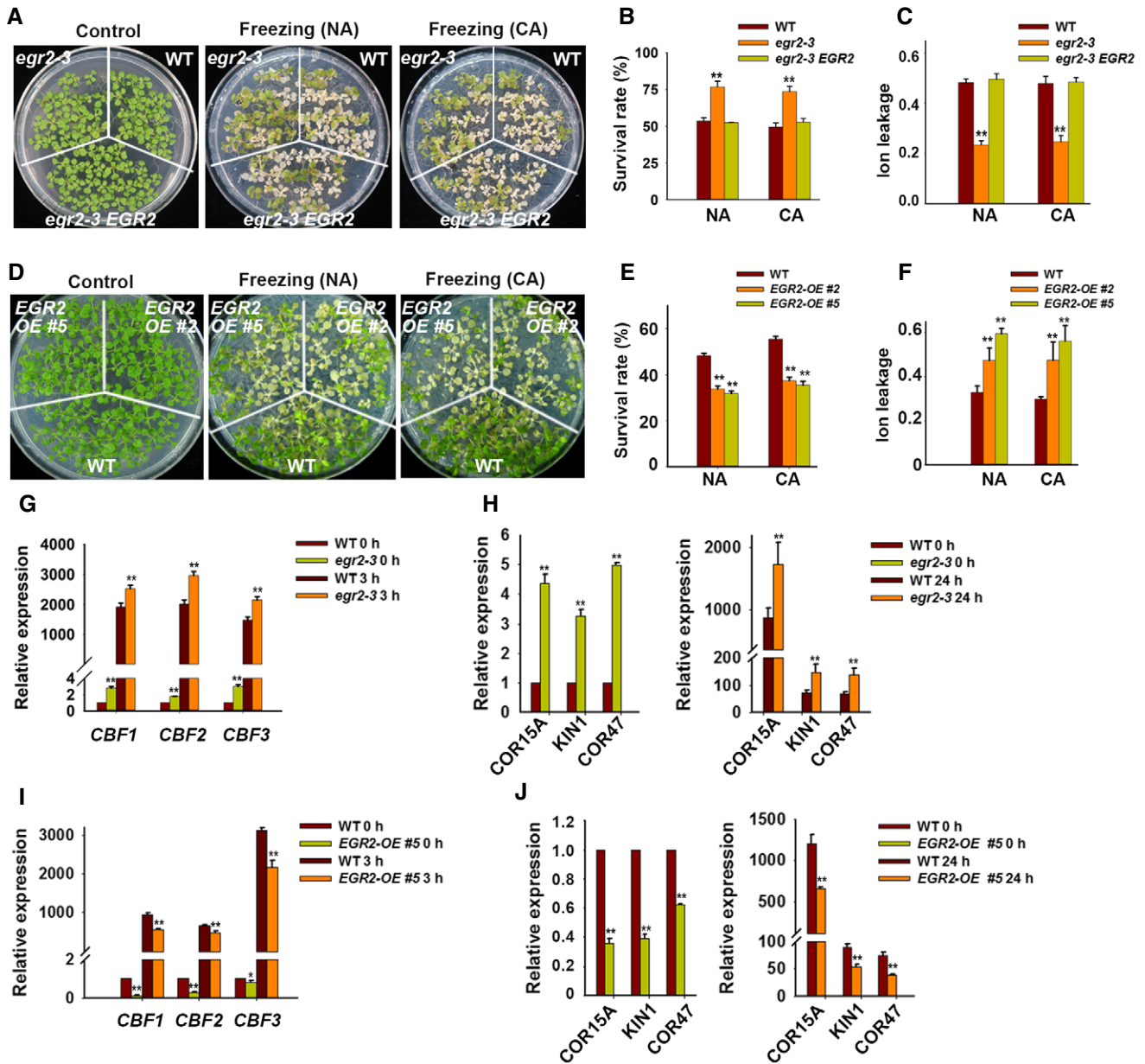
We previously showed that OST1-mediated plant freezing tolerance is dependent on the CBF signaling pathway (Ding *et al*, 2015). Therefore, we examined whether EGRs regulate the expression of *CBFs* and their target *COR* genes by qRT–PCR. The basal and cold-induced *CBF* expression was much higher in *egr1* and *egr2* mutants than that in the wild type (Figs 3G and Appendix Fig

S5M). Consistently, expression of the CBF target genes, such as *COR15A*, *KIN1*, and *COR47*, was significantly higher in *egr1* and *egr2* mutants than that in the wild type before and after cold treatment (Figs 3H and Appendix Fig S5N). By contrast, basal expression levels and cold-induced *CBF* and *COR* expression in *Super: EGR2-Myc* transgenic plants were much lower than those in the wild type (Fig 3I and J). These combined results demonstrate that EGRs inhibit OST1 activity and negatively regulate the *CBF* pathway and freezing tolerance.

EGR2 is myristoylated in plants

To gain insight into the mechanism underlying EGR2 regulation in plant freezing tolerance, we first examined whether the subcellular localization of EGR2 is affected by cold stress. EGR2 was co-localized with a plasma membrane-localized protein CPK28 (Monaghan *et al*, 2014) at the plasma membrane of *N. benthamiana* leaf pavement cells, and it was detected only in the PM fraction (Fig EV4A and B), which is consistent with a previous study (Bhaskara *et al*, 2017). However, confocal images and cell fractionation assays showed that EGR2 was not only localized at the PM, but also in the cytosol and nucleus under cold stress (Fig EV4C–E). It is worthy to note that EGR2 harbors a predicated N-terminal myristoylation motif (MGXXXS/T; Fig 4A), which is usually important for the PM localization of proteins (Hannoush, 2015). To determine whether possible myristoylation of EGR2 is responsible for its PM localization, we mutated the second amino acid Gly of EGR2 to Ala (G2A) that inhibits N-myristoylation (Ishitani *et al*, 2000), and found that EGR2^{G2A} was localized at the PM, cytosol as well as nucleus (Fig EV4F–H), which is similar to the localization of EGR2 at 4°C (Fig EV4C and E). These results indicate that the PM localization of EGR2 is affected by low temperature.

The above results imply that the possible myristoylation of EGR2 might be regulated by low temperatures. To examine whether EGR2 has myristoylated modification *in planta*, we expressed *EGR2-Myc* and *EGR2^{G2A}-Myc* in *N. benthamiana* leaves and performed an immunoblot analysis with anti-myristic acid antibody, which specifically conjugates myristic acid (Hannoush, 2015). After immunoprecipitated EGR2-Myc or EGR2^{G2A}-Myc with anti-Myc beads, myristoylated EGR2 was detected with the anti-myristic acid antibody in *N. benthamiana* leaves expressing *EGR2-Myc*, but not in leaves expressing *EGR2^{G2A}-Myc* (Fig 4B). This result indicates that EGR2 is myristoylated *in planta*. To further deeply dissect myristoylated modification of EGR2, we performed a click reaction assay which has been used in mammals and *Caenorhabditis elegans* (Fig 4C; Tang & Han, 2017). Two-week-old wild-type seedlings grown on MS medium were shifted on MS medium containing 0 or 80 μM myristic acid alkyne for additional 72 h at 22°C, and total proteins were extracted, followed by subjected to click reaction with the biotin azide at 22°C for 3 h under dark conditions. The reaction products were then separated on SDS–PAGE gel and detected with anti-streptavidin–HRP antibody. The myristoylated proteins were detected in plant materials treated with myristic acid alkyne (Fig 4D), suggesting that this method is suitable for detecting myristoylated proteins in plants. Using this approach, we prepared proteins from 2-week-old *EGR2-Myc* transgenic plants treated with the above conditions, immunoprecipitated EGR2 using anti-Myc agarose beads, and performed

Figure 3. Freezing phenotypes of *egr2-3* mutant and *EGR2*-overexpressing plants.

A–C   Freezing phenotype (A), survival rate (B), and ion leakage (C) of the *egr2-3* mutant and *egr2/EGR2:EGR2-Myc* complementation lines under non-acclimated (NA) and acclimated (CA; 4 days at 4°C) conditions. Two-week-old seedlings grown on MS medium containing 0.8% agar were treated at −5°C for 0.5 h (NA) or −8°C for 0.5 h (CA).

D–F   Freezing phenotype (D), survival rate (E), and ion leakage (F) of *EGR2*-overexpressing plants. Two-week-old *Super:EGR2-Myc* plants were treated as described in (A–C).

G–J   Expression of *CBFs* (G, I) and their target genes (H, J) in *egr2-3* mutant and *EGR2*-overexpressing plants. Two-week-old seedlings were treated at 4°C for the indicated period and subjected to qRT–PCR analysis.

Data information: In (B, C, E–J), each bar represents the mean ± SEM of three independent experiments, each of which has three technical repeats. Asterisks indicate significant differences compared to the wild type with the same treatment (*$P < 0.05$, **$P < 0.01$, two-tailed *t*-test).

immunoblot analysis with anti-streptavidin–HRP antibody. The myristoylated EGR2 was detected in *EGR2-Myc* transgenic plants treated with myristic acid alkyne (Fig 4E). Next, we tested whether N-myristoylated EGR2 was affected by low temperatures. To this end, total proteins were prepared from 2-week-old *EGR2-Myc*

seedlings treated with 4°C for 0, 3, and 6 h and immunoprecipitated by anti-Myc agarose beads. The precipitants were immunoblotted with anti-myristic acid antibody. The myristoylated form of EGR2 was detected before cold treatment, and this modification form was gradually decreased after cold treatment

Figure 4.

(Fig 4F). Together, these *in vivo* data demonstrate that EGR2 is N-myristoylated *in planta*, which is suppressed by cold stress.

To further explore the function of EGR2 N-myristoylation in plant freezing tolerance, we generated transgenic plants expressing *EGR2: EGR2^{G2A}-Myc* in *egr2-3* mutant (Fig 4G). *EGR2* fully rescued the freezing tolerance phenotype of *egr2-3* (Fig 3A–C). However, *EGR2^{G2A}-Myc* failed to complement the enhanced freezing tolerance of *egr2-3* (Fig 4H and I), suggesting that N-myristoylation of EGR2 is required for its function in regulating plant freezing tolerance.

Cold stress disrupts the interaction between NMT1 and EGR2

Next, we explored why N-myristoylated EGR2 was decreased under cold treatment. To this end, we determined whether EGR2 inter-acted with NMT1 (At5g57020), a major N-myristoyltransferase responsible for N-myristoylation in plants (Pierre *et al*, 2007). In a pull-down assay, MBP-His-EGR2, but not MBP-His, pulled down GST-NMT1 (Fig 5A), indicating that NMT1 physically interacts with EGR2 *in vitro*. Moreover, NMT1 co-localized with EGR2 at the PM

◄

of leaf pavement cells in *N. benthamiana* (Fig 5B). The interaction between NMT1 and EGR2 was further verified by a co-IP assay (Fig 5C). Furthermore, we found that the EGR2-NMT1 interaction was severely disrupted after cold treatment (Fig 5C and D). To further assess the interaction of EGR2 and NMT1 under cold stress, we immunoprecipitated EGR2 from 2-week-old *EGR2-Myc* transgenic plants treated at 4°C for 6 h and performed an *in vitro* pull-down assay. The amount of GST-NMT1 pulled down by EGR2 (4°C) was much lower than that by EGR2 (22°C; Fig 5E). All these results indicate that low temperature attenuates the formation of NMT1-EGR2 protein complex.

Mutation of *NMT1* causes late-embryo abortion (Pierre *et al*, 2007), which is impossible for freezing phenotype and related biochemical analyses. Thus, we generated transgenic plants overexpressing *NMT1* (*Super:NMT1-Myc*) to assess the function of NMT1 in plant freezing tolerance. However, the T1 transgenic seedlings highly expressing *NMT1* were seedling lethal. Therefore, we selected two independent lines expressing *NMT1* at relatively low levels, which grew normally on soil and did not show obvious morphological defects under normal growth conditions (Fig 5F), for further study. They consistently displayed reduced freezing tolerance compared to the wild type (Fig 5G and H). These plants also displayed reduced OST1 activity after cold treatment (Fig 5I and J). These combined data demonstrate that the EGR2-NMT1 interaction is impaired under low temperatures, which consequently results in the OST1 activation.

Cold stress attenuates the interaction of OST1 and EGR2

N-myristoylation is not only important for protein–membrane interaction, but also important for protein–protein interaction (Mclaughlin & Aderem, 1995; Wright *et al*, 2010). To test whether N-myristoylation of EGR2 is important for its interaction with OST1, we performed a pull-down assay using EGR2-Myc and ERG2^{G2A}-Myc proteins extracted from *EGR2:EGR2-Myc* and *EGR2:EGR2^{G2A}-Myc* stable transgenic plants. Immunoprecipitated EGR2-Myc or ERG2^{G2A}-Myc was incubated with GST-OST1 recombinant protein

and then subjected to the immunoblot analysis with anti-Myc and anti-GST antibodies, respectively. Interestingly, the interaction of EGR2^{G2A}-OST1 was much weaker than that of EGR2-OST1 (Fig 6A and B). The split luciferase complementation assay in *N. benthamiana* leaves also showed that the interaction of EGR2^{G2A}-OST1 is weak compared to that of EGR2-OST1 (Fig 6C). A co-IP assay further verified this result (Fig 6D and E). These results suggest that N-myristoylation of EGR2 is important for its interaction with OST1. Interestingly, we also found that the interaction between EGR2 and OST1 was disrupted by EGR2^{G2A} in a co-IP assay (Figure 6F and G). Low temperature inhibited EGR2 myristoylation *in planta* (Fig 4F); therefore, we performed a co-IP assay to examine whether the OST1-EGR2 interaction was affected by low temperature. OST1 was associated with EGR2 *in planta* at 22°C, and this association was significantly disrupted by cold treatment (Fig 6H and I). Next, we performed a pull-down assay to detect the interaction of EGR2 and OST1 under normal and cold conditions. EGR2-Myc proteins were extracted from 2-week-old *EGR2-Myc* stable transgenic plants treated at 4°C for 0 and 6 h and then incubated with GST-OST1. We found that the interaction of EGR2 (4°C)-OST1 was obviously reduced compared to that of EGR2 (22°C)-OST1 (Fig EV5A).

Above results indicate that cold-treated EGR2 and EGR2^{G2A} have decreased interaction ability to OST1, which prompted us to ask whether these forms of EGR2 has less activity on repressing OST1 kinase activity. To this end, we extracted EGR2-Myc (22°C) or EGR2-Myc (4°C) protein from 2-week-old *EGR2-Myc* transgenic plants treated at 4°C for 0 and 6 h and performed *in vitro* kinase assays. The results showed that OST1 kinase activity was repressed by both EGR2 (22°C) and EGR2 (4°C); however, EGR2 (4°C) had less capacity on repressing OST1 activity than EGR2 (22°C; Fig EV5B). Next, we examined the effect of EGR2^{G2A} on OST1 activity *in vitro* using immunoprecipitated EGR2^{G2A}-Myc from *EGR2^{G2A}-Myc* transgenic plants. Similar to the effect of EGR2 (4°C) on OST1, the inhibition of EGR2^{G2A} on OST1 activity was much lower than EGR2 (Fig EV5C). Intriguingly, we also found that transgenic plants overexpressing *EGR2^{G2A}-Myc* showed enhanced freezing tolerance and OST1 activity compared to the
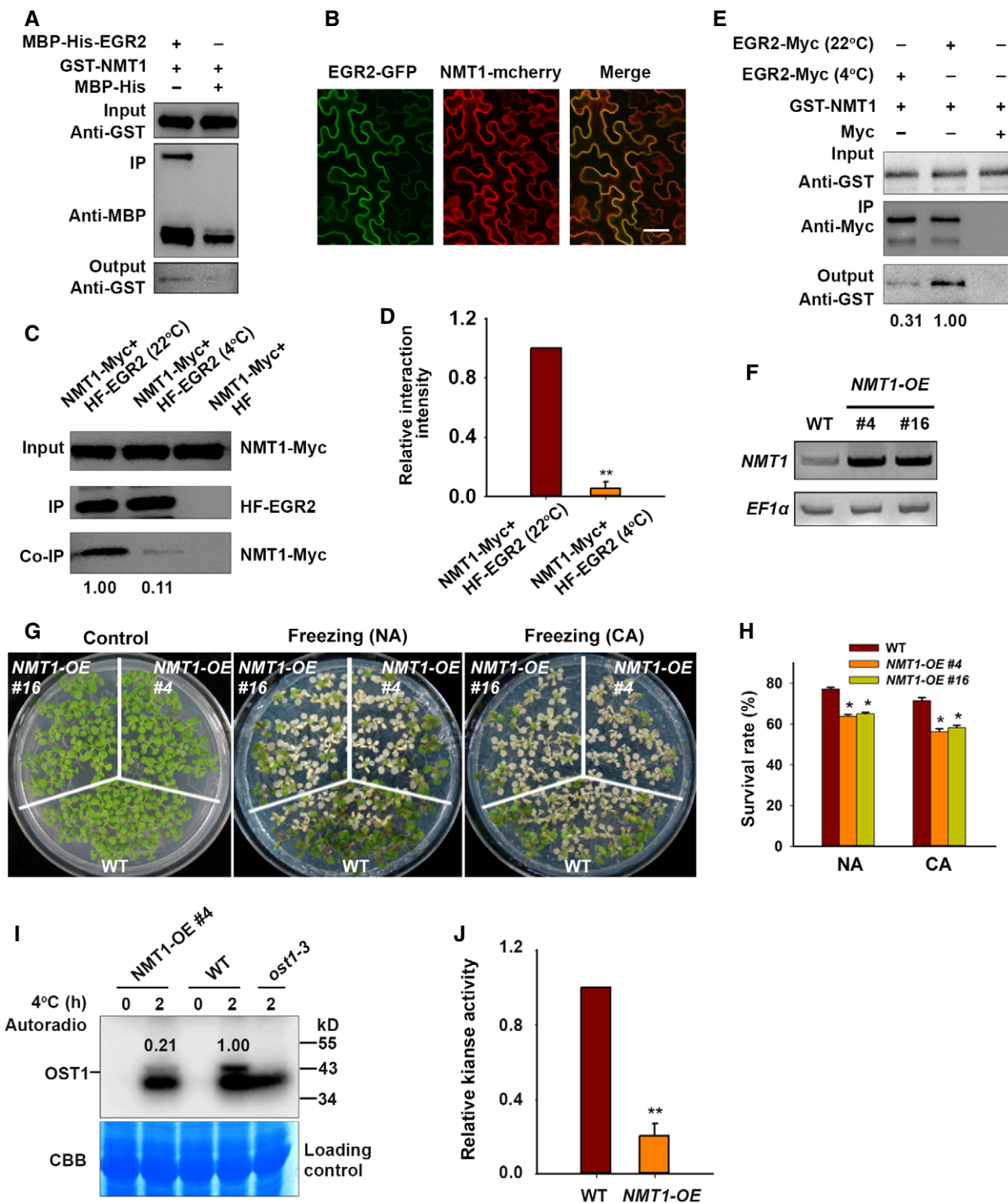
Figure 5.

wild type (Fig EV5D–F), indicating that EGR2[G2A] could prevent the inhibition of OST1 by myristoylated EGR2 *in vivo*. These combined results suggest that plants mainly synthesize unmyristoylated EGR2 under cold stress, which disrupts the formation of EGR2-OST1 protein complex, thereby activating OST1 kinase activity.

Genetic interaction of *OST1* and *EGR2*

To further determine the genetic interaction between *OST1* and *EGR2*, we crossed *ost1-3* with *egr2-3* to generate the *ost1 egr2* double mutant. The *ost1-3* mutant displayed reduced freezing tolerance, whereas the *egr2* mutant displayed enhanced freezing tolerance

Figure 5. Cold stress disrupts the interaction of NMT1 and EGR2.

A   *In vitro* pull-down assay showing the interaction of NMT1 and EGR2. Recombinant GST-NMT1 was incubated with immunoprecipitated MBP-His-EGR2 or MBP-His at 4°C for 2 h. Anti-GST and anti-MBP were used to detect NMT1, EGR2, and MBP-His, respectively.

B   Co-localization of NMT1 and EGR2 in *N. benthamiana* leaves. Scale bar: 50 μm.

C, D   Effect of cold stress on the interaction of EGR2 and NMT1 determined by co-IP assay. *Arabidopsis* protoplasts expressing *HF/NMT1-Myc* and *HF-EGR2/NMT1-Myc* were treated with or without 4°C for 2 h. Total proteins were immunoprecipitated by anti-HA agarose beads. Anti-Myc and anti-HA were used to detect NMT1-Myc and HF-EGR2, respectively. In (C), relative band intensity is shown below the co-IP blot. In (D), each bar represents the mean ± SEM of three biological experiments (**$P < 0.01$, two-tailed *t*-test).

E   *In vitro* pull-down assay showing decreased interaction intensity of EGR2 (4°C) and NMT1 compared with that of EGR2 (22°C) and NMT1. Total proteins prepared from 2-week-old EGR2-Myc plants grown at 4°C for 0 and 6 h were immunoprecipitated by anti-Myc agarose beads and incubated with GST-NMT1 in pull-down buffer for 2 h at 4°C. Anti-Myc and anti-GST antibodies were used to detect EGR2 and NMT1 proteins. Relative band intensity is shown below the output blot.

F   Expression of *NMT1* in *NMT1-Myc*-overexpressing plants. *EF1α* was used as a loading control.

G, H   Freezing phenotype (G) and survival rate (H) of *NMT1-Myc*-overexpressing transgenic plants. Two-week-old *Super:NMT1-Myc* plants were treated at −5°C (NA) or −8°C for 0.5 h (CA). In (H), each bar represents the mean ± SEM of three biological experiments, and asterisks indicate significant differences compared with the wild type for the same treatment (*$P < 0.05$, two-tailed *t*-test).

I, J   OST1 kinase activity in *NMT1-Myc*-overexpressing plants under cold stress. Top, autoradiograph; bottom, CBB staining. Representative pictures are shown in (I), and the relative kinase activity is shown in (J). In (I), the ratio of band intensity of OST1 to RuBisCO in wild type with cold treatment for 2 h was set to 1.00. In (J), each bar represents the mean ± SEM of three independent experiments (**$P < 0.01$, two-tailed *t*-test).

Source data are available online for this figure.

(Fig 7A). The *ost1 egr2* double mutant phenocopied the *ost1* single mutant in terms of survival rate and ion leakage (Fig 7B).

We also evaluated the expression levels of *CBF*s in wild-type, *ost1-3*, *egr2-3*, and *ost1 egr2* plants. The expression of *CBF*s in *ost1 egr2* resembled *ost1*, both much lower than the wild type before and after cold treatment (Fig 7C). These combined results indicate that *EGR2* acts upstream of *OST1* to negatively regulate *CBF* expression and freezing tolerance.

Discussion

We previously identified OST1 as a key protein kinase that positively regulates plant freezing tolerance (Ding *et al*, 2015). In the present study, we found that EGR2 interacts with OST1 and inhibits OST1 kinase activity *in vitro* and *in vivo* at 22°C. EGR2 has N-myristoylated modification catalyzed by *Arabidopsis* N-myristoyltransferase NMT1 under normal conditions, which promotes EGR2-OST1 protein complex formation. Under cold stress, the interaction of NMT1 and EGR2 is compromised, causing the accumulation of newly synthesized unmyristoylated EGR2, which dissociates from OST1 and competes for the interaction of myristoylated EGR2 and OST1. As a result, OST1 is activated, thereby promoting *CBF* expression and freezing tolerance in *Arabidopsis* (Fig 7D).

In both eukaryotes and prokaryotes, PP2Cs usually cooperate with sensor proteins to respond to changes in environmental cues throughout the life cycle (Fuchs *et al*, 2013). Energy sensor RsbQ and the PP2C RsbP regulate energy and nutritional response in *B. subtilis* (Martinez *et al*, 2010). Dynamic regulation of clade-A PP2Cs with ABA receptors PYR/PYL/RCAR and ABA is required for downstream protein kinase activation to confer plant ABA response (Ma *et al*, 2009; Park *et al*, 2009; Yin *et al*, 2009). In the present study, we found that PP2C-type clade-E phosphatase EGR2 negatively regulates plant freezing tolerance by repressing OST1 kinase activity. Although this negative regulation is repressed by low temperature, expression of *EGR2* gene is up-regulated by low temperature (Appendix Fig S1A). This phenomenon is reminiscent of ABA signaling, in which group A *PP2Cs* is induced by ABA, but their ability for repressing OST1 activity is inhibited by ABA (Fujii

et al, 2009; Nakashima & Yamaguchi-Shinozaki, 2013). It appears a feedback regulation in plant responses to adverse conditions. Despite the induction of *EGR2* gene, cold-induced unmyristoylated EGR2 is mainly synthesized, which shows low binding ability to OST1 and thus releases the inhibition of EGR2 on OST1 under cold conditions.

Clade-A PP2Cs, such as ABI1 and ABI2, are also responsible for repressing cold-induced OST1 activity (Ding *et al*, 2015; Fig 1C and D). In the ABA signaling pathway, the function of ABI1 on inhibiting OST1 kinase activity is repressed by ABA and ABA receptors (Fujii *et al*, 2009). However, we showed that cold-activated OST1 activity is not dependent on ABA and ABA receptors (Ding *et al*, 2015; Fig 1A and B). Thus, it is unlikely that the release of OST1 by ABI1 is coupled with ABA or ABA receptors under cold stress. The mechanism of OST1 activation mediated by ABI1 under cold stress needs further investigation. It is noteworthy that cold-induction of OST1 activity is approximately ninefold in *egr1 egr2* double mutant, whereas it is reduced to half level in *EGR2*-overexpressing lines when compared to the WT in in-gel kinase assay (Fig 2F–I). In contrast, OST1 activity is 30% less in *ABI1*-overexpressing line than the WT but twofold in *abi1 abi2 hab1* mutant compared to WT (Fig 1C and D). These results suggest that clade-E PP2C EGRs and clade-A PP2Cs in parallel or coordinately regulate OST1 activity at/around the PM, and in the cytosol and nucleus, respectively. Compared to ABI1/2, EGRs play a predominant role to modulate OST1 activity in response to cold stress.

Intriguingly, we found that the EGR2 phosphatase is localized at the PM under warm temperatures, but at the PM, cytosol, and nucleus under cold stress (Fig EV4). Lipid modification of proteins, such as myristoylation and palmitoylation, is important for PM localization in plants (Hannoush, 2015). We found that EGR2 is N-myristoylated *in planta*, and it is partially responsible for the PM localization of EGR2 (Figs 4 and EV4). Moreover, N-myristoylation is also important for protein–protein interactions (Mclaughlin & Aderem, 1995; Wright *et al*, 2010). It is possible that N-myristoylation on EGR2 may be involved in its interaction with other proteins. Interestingly, N-myristoylation of EGR2 is important for its interaction with OST1 in plants. It is likely that protein conformation of myristoylated EGR2 is suitable for recognizing its target proteins.
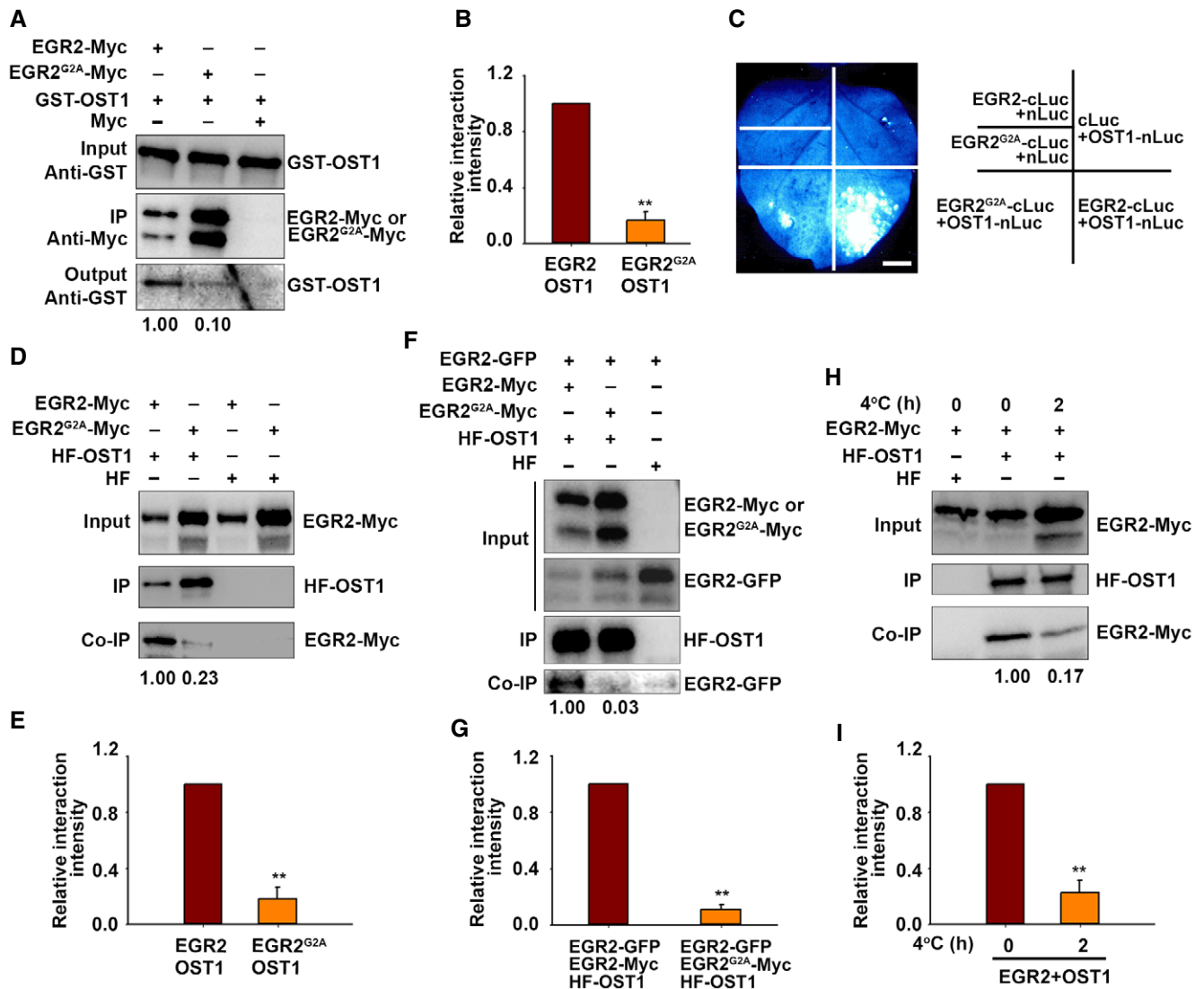
Figure 6. Cold stress attenuates the interaction between EGR2 and OST1.

A, B   Pull-down assay. Total proteins prepared from *EGR2-Myc* or *EGR2^G2A^-Myc* transgenic plants were immunoprecipitated with anti-Myc agarose beads and then incubated with GST-OST1. Anti-Myc and anti-GST antibody were used to detect GST-OST1 and EGE2-Myc. Representative pictures are shown in (A). Relative interaction is shown in (B).

C   LCI of EGR2 and EGR2^G2A^ with OST1 in *N. benthamiana* leaves. *EGR2-cLuc/OST1-nLuc* and *EGR2^G2A^-cLuc/OST1-nLuc* were expressed in *N. benthamiana* leaves for 48 h. *EGR2-cLuc/nLuc*, *EGR2^G2A^-cLuc/nLuc*, and *cLuc/OST1-nLuc* were used as negative controls. Scale bar: 2 cm.

D, E   Co-IP assay. *EGR2-Myc/HF-OST1*, *EGR2^G2A^-Myc/HF-OST1*, *HF/EGR2-Myc*, and *HF/EGR2^G2A^-Myc* were expressed in *N. benthamiana* leaves. Total proteins were immunoprecipitated by anti-HA agarose beads. Anti-HA and anti-Myc antibodies were used to detect HF-OST1, EGR2-Myc, and EGR2^G2A^-Myc, respectively. Representative pictures are shown in (D), and relative interaction is shown in (E).

F, G   Effect of EGR2^G2A^ on the interaction of OST1 and EGR2 in *Arabidopsis* protoplasts expressing *HF-OST1/EGR2-GFP/EGR2-Myc*, *HF-OST1/EGR2-GFP/EGR2^G2A^-Myc*, or *HF-OST1/EGR2-GFP*. Total proteins were immunoprecipitated by anti-HA agarose beads. Anti-Myc, anti-GFP, and anti-HA antibodies were used to detect EGR2-Myc, EGR2-GFP, and HF-OST1, respectively. Representative pictures are shown in (F), and relative interaction is shown in (G).

H, I   Effect of cold stress on the interaction of OST1 and EGR2. *Arabidopsis* protoplasts expressing *EGR2-Myc/HF-OST1* and *EGR2-Myc/HF* were treated at 4°C for 0 and 2 h. Total proteins were immunoprecipitated by anti-HA agarose beads. The co-immunoprecipitated products were detected by anti-HA and anti-Myc antibodies, respectively. Representative pictures are shown in (H), and the relative interaction is shown in (I).

Data information: In (A, D, F, and H), relative band intensities are shown. In (B, E, G and I), each bar represents the mean ± SEM of three independent experiments (**$P < 0.01$, two-tailed *t*-test).

Source data are available online for this figure.

This possibility was hypothesized from some examples in animals. For instance, activation of ADP ribosylation factor (ARF) GTPase in animals requires its membrane localization conferred by N-myristoylation, and the protein conformation of ARFs allows ARF-GTP to be an active form that has increased affinity for multiple effectors, thereby initiating some cellular and physiological
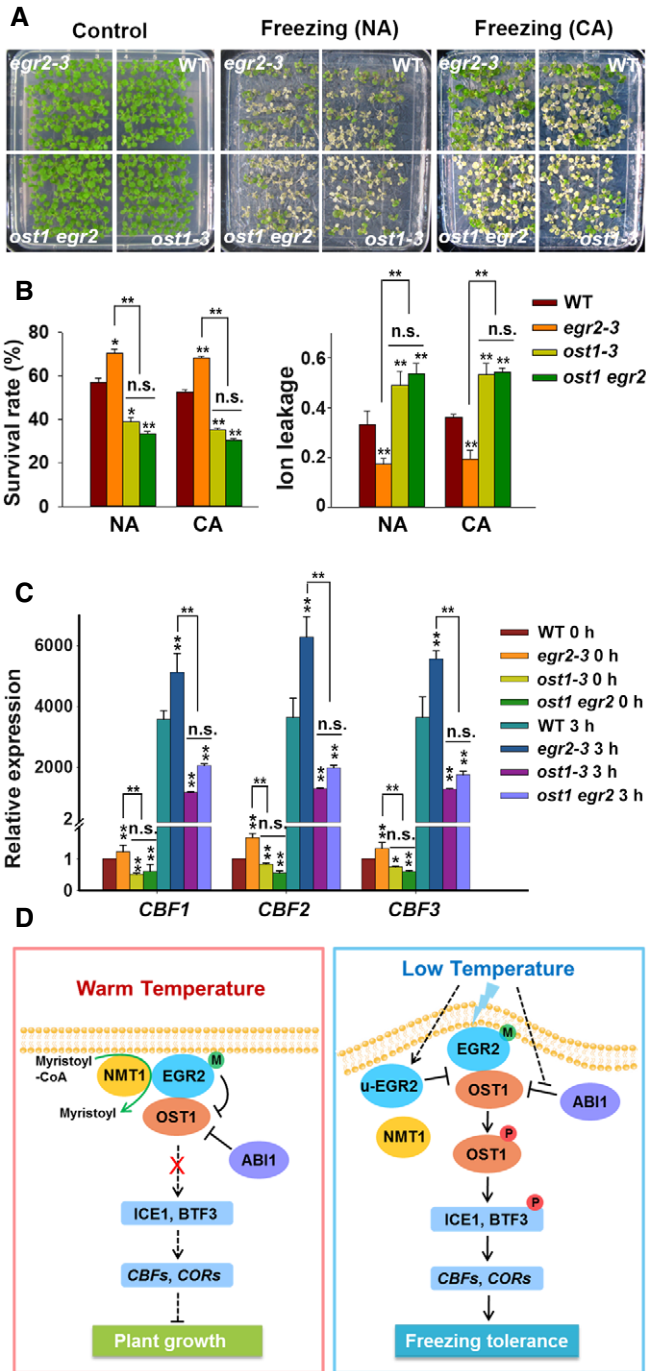
Figure 7. Genetic Interaction of *OST1* and *EGR2*.

A, B   Freezing phenotype (A), survival rate and ion leakage (B) of wild-type, *ost1-3*, *egr2-3*, and *ost1 egr2* mutants. Two-week-old seedlings grown on MS medium were treated at −5°C (NA) or −8°C for 0.5 h (CA).

C   Expression of *CBF*s in wild-type, *ost1-3*, *egr2-3*, and *ost1 egr2-3* plants under cold stress. Two-week-old seedlings grown at 22°C were treated at 4°C for 0 and 3 h.

D   Model of EGR2-OST1 modulation of cold stress responses in *Arabidopsis*. At warm temperature (22°C), EGR2 can be modified by myristoylation, which allows it to recognize OST1 and inhibit its activity to ensure plant growth. Under cold stress (4°C), the interaction of NMT1 and EGR2 is decreased, thereby causing the accumulation of unmyristoylated EGR2, which shows reduced interaction with OST1 and disrupts the interaction of EGR2-OST1 as well. This ultimately leads to activating OST1 protein kinases and enhancing plant freezing tolerance. Clade-A PP2Cs, such as ABI1, also partially contributes to regulating OST1 activity in response to cold stress. EGR2-M and u-EGR2 represent myristoylated and unmyristoylated EGR2, respectively.

Data information: In (B, C), each bar represents the mean ± SEM of three independent experiments, each of which has three technical repeats. Asterisks indicate significant differences compared to the wild type with the same treatment (*$P < 0.05$, **$P < 0.01$, two-tailed *t*-test).

EGR2 is likely sufficient but unnecessary for its interaction with OST1. However, we cannot rule out the other possibility: Protein conformation of EGR2 for recognizing its substrates in *E. coli* and plants is different.

Our result showed that N-myristoylated EGR2 is gradually decreased after 3 h and 6 h of cold treatment (Fig 4), which activates OST1 followed by stabilizing ICE1. Therefore, it is expected that *CBF* expression still keeps high level at 6 h after cold treatment. However, the expression of *CBF* genes peaks at 3 h after cold treatment and gradually reduces later. This phenomenon supports the notion that in addition to OST1-ICE1 module as positive regulators, some other negative regulators are involved in regulating *CBF* gene expression, such as PIFs (Lee & Thomashow, 2012; Jiang *et al*, 2017), MYB15 (Agarwal *et al*, 2006), and EIN3 (Shi *et al*, 2012), so that plants adjust an appropriate cold response to balance plant growth and cold tolerance.

PM-localized proteins are involved in sensing and transducing signals into the cell, thereby activating subsequent cellular responses (de Mendoza, 2014). In *Oryza sativa* (rice), the COLD1 protein located at the PM and endoplasmic reticulum membrane may sense cold signal and activate chilling tolerance responses (Ma *et al*, 2015). In *B. subtilis*, the PM-localized protein histidine kinase DesK functions as a cold sensor with characteristic bifunctional enzyme activities (containing both kinase and phosphatase activities; Albanesi *et al*, 2009; Cybulski *et al*, 2015). DesK protein structures differ under different temperature conditions; these structures correspond with its bifunctional enzyme activities (Cybulski *et al*, 2015). We hypothesized that higher plants might have evolved a specialized protein or protein complex that regulates responses to extreme environmental temperatures, in a manner similar to DesK in *B. subtilis*. N-myristoylation is an evolutionarily conserved mechanism of protein post-translational modification (Farazi *et al*, 2001). The myristoyl group of protein fosters protein–protein and protein–membrane interactions and stabilizes protein conformation (Mclaughlin & Aderem, 1995; Wright *et al*, 2010). This so-called myristoyl switch makes it an essential feature of many cellular processes and signal transduction pathways, such as proliferation,

processes (Goldberg, 1998; Wright *et al*, 2010). More importantly, EGR2-NMT1 interaction is weakened under cold stress, which consequently leads to production of more unmyristoylated EGR2 in plants (Fig 5). The possible conformation change from myristoylated to unmyristoylated form renders attenuated association of EGR2 and OST1, thereby releasing OST1 inhibition under cold stress. It is worthy to note that EGR2 purified from *E. coli* (in which myristoylated modification does not exist) also interacts with OST1. Given that the interaction of EGR2^{G2A} (purified from plants) and OST1 is not fully dissociated, the myristoylated modification on

differentiation, and disease resistance in human (Wright *et al*, 2010). Thus, we postulate that myristoyl switch on the PM-localized EGR2 may be involved in cold perception and transduction of plants. Under normal temperatures, myristoylated EGR2 interacts with and dephosphorylates OST1, which keeps the stress response at "off" state, ensuring plant growth and development. Under cold conditions, N-myristoylation of EGR2 is at "off" state, which fosters activation of OST1-mediated cold stress response, leading to enhanced freezing tolerance in plants (Fig 7D).

Materials and Methods

Plants materials and growth conditions

The *Arabidopsis thaliana* Col-0 ecotype was used in this study, and the plants were grown on soil or Murashige and Skoog (MS) medium (Sigma-Aldrich) containing 0.8% agar and 2% sugar under long-day conditions (16-h light/8-h dark) at 22°C. The mutants *ost1-3/snrk2.6* (Salk_008068; Ding *et al*, 2015), *egr1-1* (Salk_011589), *egr1-2* (GK-013B05), *egr2-1* (Salk_048861), *egr2-3* (Salk_0424824), *egr3-1* (Salk_061302), and *egr3-2* (Salk_132380) were obtained from the *Arabidopsis* Biological Resource Center.

Plasmid construction and plant transformation

EGR2 cDNA was amplified and cloned into *pSuper1300* (Ni *et al*, 1995; Yang *et al*, 2010), *pGEX4T-1*, *pMalC2*, and *pGADT7* vectors to obtain *Super:EGR2-Myc*, *Super:EGR2-GFP*, *GST/MBP-His-EGR2*, *EGR2-pGADT* constructs, respectively.

 EGR2 promoter together with genomic DNA amplified by PCR was fused with GFP or Myc in the *pCAMBIA1300* vector to generate *EGR2:EGR2-Myc* vector.

 Mutated forms of EGR2 were obtained by site-directed mutagenesis using *EGR2* genomic DNA as templates, and then amplified by PCR. They were cloned into *pSuper1300* or *pCAMBIA1300* vectors to generate *Super:EGR2^{G2A}-Myc, Super:EGR2^{G2A}-GFP* and *EGR2: EGR2^{G2A}-Myc* vectors.

 EGR1 and *EGR3* cDNAs were amplified and cloned into *pSuper1300* vector to generate *Super:EGR1-Myc* and *Super:EGR3-Myc*.

 NMT1 cDNA was amplified and cloned into *pSuper1300* and *pGEX4T-1* vectors to generate *Super:NMT1-Myc* and *GST-NMT1* constructs, respectively.

 SnRK2.2 and *SnRK2.3* cDNAs were amplified and cloned into *pCM1307* and *pGEX4T-1* vectors to generate *HF-SnRK2.2/HF-SnRK2.3* and *GST-SnRK2.2/GST-SnRK2.3* constructs, respectively.

 OST1 cDNA was amplified and cloned into *pCM1307* vector to generate *HF-OST1* construct, respectively. All primers used in vector construction are listed in Appendix Table S2.

 All transgenic plants were generated through *Agrobacterium*-mediated transformation by floral dip (Clough & Bent, 1998), and selected by hygromycin B. T4 homozygous transgenic plants were used in this study.

Freezing tolerance and ion leakage assays

The freezing tolerance was performed as described (Ding *et al*, 2015). Briefly, plants were grown on MS plates containing 0.8%

agar and 2% sugar at 22°C for 2 weeks and transferred to 4°C chamber for 4 days as cold acclimation, or directly subjected to freezing treatment in a freezer chamber (RUMED4501). The freezing program was set at 0°C and dropped 1°C/h to desired temperatures. After freezing treatment, the seedlings were transferred to 4°C for 12 h at dark condition and then put into normal conditions for recovery for 3 days and the number of seedlings that generated new leaves was counted for survival rate. After freezing treatment, the injured seedlings were subjected to the ion leakage assay as described (Ding *et al*, 2015).

Gene expression assays

Total RNA was extracted from 14-day-old seedlings with or without cold treatment using TRI Reagent (Thermo Fisher Scientific) and reverse-transcribed using the M-MLV Reverse Transcriptase (Promega). Quantitative real-time PCR was performed using Applied Biosystems 7500 Real-Time PCR system with SYBR Premix Ex *Taq* (Takara). The expression of various genes was calculated as previously described (Shi *et al*, 2012). The expression of *actin2* was used as an internal control. The primers used for gene expression were listed in Appendix Table S2.

Protein expression and purification from *E. coli*

To obtain purified EGR2 and OST1 proteins, His-OST1, MBP-His-EGR2, GST-OST1, GST-SnRK2.2/GST-SnRK2.3, and GST-EGR2 plasmids were transformed into *E. coli* (BL21), and then induced by 0.5 mM IPTG at 18°C for 12 h. The expressed recombinant proteins were affinity-purified using nickel nitriloacetic acid and glutathione-linked resins according to the protocols (GE). The purified proteins were used in pull-down and *in vitro* protein kinase assays.

Yeast two-hybrid assays

The yeast two-hybrid assay was performed as described (Ding *et al*, 2015). In brief, OST1-pGBKT7 and EGR2-pGADT7, OST1-pGBKT7 and pGADT7 or pGBKT7 and EGR2-pGADT7 were transformed into yeast strain AH109. The yeast cells were grown on SC/–Leu/−Trp (Clontech, #630417; 3 days) or SC/−Leu/−Trp/−His/−Ade medium (Clontech, #630428) for 6 days.

In vitro pull-down assays

For pull-down assay, 5 μg purified MBP-His-EGR2 or MBP-His proteins was incubated with MBP agarose beads (GE Healthcare, #71502076-EG) in PBS buffer containing 0.1% NP-40 (pull-down buffer) for 2 h at 4°C and then washed by PBS buffer for three times. The immunoprecipitated MBP-His-EGR2 or MBP-His was incubated with 0.5 μg GST-OST1 for 2 h at 4°C in pull-down buffer. The proteins were washed by PBS buffer for five times and separated by SDS–PAGE. Anti-His (Beijing Protein Innovation, #AbM59012-18-PU) and anti-GST antibodies (Beijing Protein Innovation, #AbM59001-2H5-PU) were used to detect MBP-His-EGR2, MBP-His, and GST-OST1, respectively.

 For detecting the interaction of NMT1 and EGR2, 0.5 μg GST-NMT1 incubated with the immunoprecipitated MBP-His-EGR2 or MBP-His (5 μg) by MBP agarose beads (GE Healthcare, #71502076-EG).

The proteins were washed by PBS buffer for five times and separated by SDS–PAGE. Anti-His (Beijing Protein Innovation, #AbM59012-18-PU) and anti-GST antibodies (Beijing Protein Innovation, #AbM59001-2H5-PU) were used to detect MBP-His-EGR2, MBP-His, and GST-NMT1, respectively.

To dissect the interaction of SnRK2.2 and EGR2 or SnRK2.3 and EGR2, the immunoprecipitated MBP-His-EGR2 or MBP-His (5 μg) by MBP agarose beads (GE Healthcare, #71502076-EG) was incubated with 0.5 μg GST-SnRK2.2 or GST-SnRK2.3 in pull-down buffer for 2 h. The precipitants were washed with PBS buffer for five times and then separated by SDS–PAGE. EGR2, SnRK2.2, and SnRK2.3 were detected with anti-His (Beijing Protein Innovation, #AbM59012-18-PU) and anti-GST antibodies (Beijing Protein Innovation, #AbM59001-2H5-PU).

To analyze the interaction of EGR2[G2A] and OST1, immunoprecipitated EGR2[G2A] protein prepared from 2-week-old EGR2[G2A]-Myc transgenic plants was incubated with 1 μg GST-OST1 in pull-down buffer for 2 h. After five times washing with PBS buffer, the proteins were separated by SDS–PAGE and detected by anti-Myc (Sigma-Aldrich, #M4439) and anti-GST (Beijing Protein Innovation, #AbM59001-2H5-PU) antibodies.

To detect the interaction of EGR2 (4°C) and OST1, EGR2-Myc (4°C) protein extracted from 2-week-old *EGR2-Myc* plants treated at 4°C for 6 h was immunoprecipitated by anti-Myc agarose beads for 2 h at 4°C and then incubated with 1 μg GST-OST1 in pull-down buffer for additional 2 h at 4°C. Immunoprecipitated proteins were washed five times with PBS buffer and then separated by SDS–PAGE. Anti-Myc (Sigma-Aldrich, #M4439) and anti-GST (Beijing Protein Innovation, #AbM59001-2H5-PU) antibodies were used to detect EGR2 and OST1 proteins. The same method was used to examine the interaction of EGR2 (4°C) and NMT1.

Co-IP assays

Co-IP assay was performed as previously described (Ding *et al*, 2015). In brief, the total proteins were extracted from *N. benthamiana* leaves expressing *35S:HF-OST1/Super:EGR2-Myc,* or *35S:HF-OST1/Super:Myc* constructs with protein extraction buffer (2 mM EDTA pH 8.0, 50 mM Tris–HCl pH 7.5, 150 mM NaCl, 0.1% NP-40, and 0.1% Triton X-100) and then incubated with anti-Myc agarose (Sigma-Aldrich, #A7470) for 2 h at 4°C. After washing by extraction buffer for five times, the co-immunoprecipitated products were separated by SDS–PAGE and detected with anti-Myc (Sigma-Aldrich, #M4439) and anti-HA (Sigma-Aldrich, #H3663) antibodies. The same method was used to examine the interaction of EGR1/OST1 and EGR3/OST1.

For the NMT1 and EGR2 interaction assay, proteins were prepared from *Arabidopsis* protoplasts expressing *Super:NMT1-Myc/35S:HF-EGR2* and *Super:NMT1-Myc/35S:HF* with or without cold treatment for 2 h. The proteins were extracted and incubated by anti-HA agarose at 4°C for 2 h and detected with anti-Myc (Sigma-Aldrich, #M4439) and anti-HA antibodies (Sigma-Aldrich, #H3663).

For the interaction of OST1 and EGR2 under cold stress, *35S:HF-OST1/Super:EGR2-Myc* or *35S:HF/SuperEGR2-Myc* plasmids were transformed into *Arabidopsis* protoplasts and expressed for 16 h and then treated at 4°C for 2 h. Proteins were extracted and incubated by anti-HA agarose (Sigma-Aldrich, #A2095) at 4°C for 2 h and detected with anti-HA (Sigma-Aldrich, #H3663) and anti-Myc antibodies (Sigma-Aldrich, #M4439).

For the interaction of SnRK2.2 and EGR2, HF-SnRK2.2/EGR2-Myc or HF/EGR2-Myc proteins were expressed in *N. benthamiana* leaves for 48 h. Total proteins were extracted with protein extraction buffer and incubated with anti-HA agarose (Sigma-Aldrich, #A2095) at 4°C for 2 h. The immunoprecipitated products were separated by SDS–PAGE and detected by anti-HA (Sigma-Aldrich, #H3663) and anti-Myc (Sigma-Aldrich, #M4439) antibodies. The same method was used to examine the interaction between SnRK2.3 and EGR2.

Protein kinase assays

In vitro kinase assay was performed as previously described (Ding *et al*, 2015). Purified recombinant protein combinations (His-OST1/MBP-His-EGR2, His-OST1/MBP-His) were incubated with kinase reaction buffer containing 20 mM MgCl$_2$, 20 mM Tris–HCl pH 7.5, 1 mM DTT, 50 μM ATP, and 1 μCi [γ-^{32}P]ATP at 30°C for 30 min and then heated at 100°C for 5 min with 5× loading buffer. The proteins were separated by SDS–PAGE and detected by Typhoon 9410 imager.

For in-gel kinase assay, total proteins were extracted from 10-day-old seedlings grown at 22°C at long-day conditions with or without cold treatment with protein extraction buffer containing 5 mM EDTA, 5 mM EGTA, 5 mM DTT, 25 mM NaF, 1 mM Na$_3$VO$_4$, 20% glycerol, 1 mM phenylmethylsulfonyl fluoride, 1× protease inhibitor cocktail (Roche), and 50 mM HEPES-KOH, pH 7.5. Proteins were separated on a SDS–PAGE gel containing 0.1 mg/ml GST-ΔABF2 substrate. After washing by washing buffer (1 mM DTT, 5 mM NaF, 0.1 mM Na$_3$VO$_4$, 0.5 mg/ml BSA, 0.1% Triton X-100, and 25 mM Tris–HCl, pH 7.5) for three times, 20 min each, the gel was renatured with buffer containing 2 mM DTT, 5 mM NaF, 0.1 mM Na$_3$VO$_4$, and 25 mM Tris–HCl, pH 7.5, for 1, 12, and 1 h at 4°C. Then, the gel was incubated with kinase reaction buffer (2 mM EGTA, 12 mM MgCl$_2$, 1 mM DTT, 0.1 mM Na$_3$VO$_4$, and 25 mM HEPES-KOH, pH 7.5) for 30 min, and then incubated with reaction buffer supplemented with 60 μCi [γ-^{32}P]ATP and 9 μl 1 mM cold ATP at room temperature for 1.5 h. The gel was washed by 5% TCA and 1% sodium pyrophosphate five times for 30 min each. The signal was detected by Typhoon 9410 imager.

Cell fractionation assays

The details for plasma membrane fractionation were performed as described (Liu *et al*, 2017) with some modifications. Briefly, total proteins were prepared from 2-week-old seedlings of *EGR2:EGR2-Myc* or *EGR2:EGR2[G2A]-Myc* treated at 4°C for 0 and 6 h with 200 μl protein extraction buffer and filtered through Miracloth (Calbiochem) and 20 μl solution was saved as total protein fraction. The remainder was centrifuged at 5,000 *g* for 5 min to remove organelles and debris. Supernatants were centrifuged at 100,000 *g* for 1.5 h at 4°C to separate soluble and membrane fractions. Supernatants were used for the soluble sample. Membrane pellets were resolved in 180 μl protein extraction buffer. Anti-Myc (Sigma-Aldrich, #M4439) was used to detect EGR2 and EGR2[G2A] proteins. Anti-PEPC (Agrisera, #AS09 458; RRID: AB_1312) and anti-GHR1 (produced from Shanghai Youke Biotech Co., LTD) antibodies were used to detect the cytosolic and plasma membrane proteins.

The procedure for nucleus/cytosolic proteins fractionation assays was followed according to the protocol of CelLytic PN Isolation/Extraction kit (Sigma-Aldrich, #CELLYTPN1). Briefly, total proteins were prepared from 2-week-old seedlings of *EGR2:EGR2-Myc* or *EGR2:EGR2^{G2A}-Myc* treated with or without low temperature 400 μl protein extraction buffer and incubated on ice for 20 min and filtered through Miracloth (Calbiochem), and 40 μl solution was saved as total protein. The protein was centrifuged at 12,000 *g* for 10 min, and supernatant was transferred into other 1.5-ml tube as soluble fraction. The sediment was washed by protein extraction buffer for five times, five min each, and then resolved by 40 μl nuclear protein extraction buffer. Anti-OST1 (produced from Shanghai Youke Biotech Co., LTD) was used to detect OST1 protein. Anti-PEPC (Agrisera, #AS09 458; RRID: AB_1312) and anti-H3 (Millipore, #05-499; RRID: AB_2787688) antibodies were used to detect the cytosolic and nucleus proteins, respectively.

Analysis of EGR2 myristoylation

The protocol for detecting myristoylated EGR2 in plant was modified from previous study (Tang & Han, 2017). Briefly, 2-week-old seedlings grown on MS medium were treated with or without 80 μM myristic acid alkyne (Cayman Chemical, #13267) at 22°C for additional 72 h. Total proteins were prepared with lysis buffer and subjected to click reaction with click reaction kit (Click Chemistry Tools, #1001) and biotin azide (PEG4 carboxamide-6-azidohexanyl biotin, Invitrogen, #B10184). The reaction products were immunoprecipitated with anti-Myc agarose beads (Sigma-Aldrich, #A7470) and separated on SDS–PAGE. Streptavidin–HRP (CST, #3999) was used for detecting biotin-labeled proteins.

LC-MS/MS analysis

The details of LC-MS/MS for searching interacting proteins were performed as described (Liu *et al*, 2017) with some modifications. Total proteins (50 mg) were prepared from *EGR2-Myc* transgenic plants with protein extraction buffer (50 mM Tris–HCl pH 7.5, 2 mM EDTA pH 8.0, 150 mM NaCl, 20% glycerol, 0.5% Triton X-100, 0.1% NP-40) and immunoprecipitated with anti-Myc agarose (Sigma-Aldrich, #A7470). The precipitants were washed by 1 ml protein extraction buffer for five times, four min each, and then eluted by 0.1 M glycine-HCl (pH 2.8) and neutralized by 1 M Tris buffer. The elution products were dissolved in NH_4HCO_3 solution (30 ml, 50 mM) and reduced with DTT and alkylated with IAM. The reaction products were digested by trypsin (pH 8.5) at 37°C for 12 h and then diluted with 0.1% formic acid, and centrifuged at 15,294 *g* for 20 min. The supernatant was collected for nanoLC-MS analysis with a Thermo Q-Exactive high-resolution mass spectrometer (Thermo Scientific). The putative interacting proteins of EGR2 and search parameters are listed in Appendix Table S1.

Expanded View for this article is available online.

References

Agarwal M, Hao YJ, Kapoor A, Dong CH, Fujii H, Zheng XW, Zhu JK (2006) A R2R3 type MYB transcription factor is involved in the cold regulation of CBF genes and in acquired freezing tolerance. *J Biol Chem* 281: 37636–37645

Aguilar PS, Hernandez-Arriaga AM, Cybulski LE, Erazo AC, de Mendoza D (2001) Molecular basis of thermosensing: a two-component signal transduction thermometer in *Bacillus subtilis*. *EMBO J* 20: 1681–1691

Albanesi D, Mansilla MC, de Mendoza D (2004) The membrane fluidity sensor DesK of *Bacillus subtilis* controls the signal decay of its cognate response regulator. *J Bacteriol* 186: 2655–2663

Albanesi D, Martin M, Trajtenberg F, Mansilla MC, Haouz A, Alzari PM, de Mendoza D, Buschiazzo A (2009) Structural plasticity and catalysis regulation of a thermosensor histidine kinase. *Proc Natl Acad Sci USA* 106: 16185–16190

Bhaskara GB, Wen TN, Nguyen TT, Verslues PE (2017) Protein phosphatase 2Cs and microtubule-associated stress protein 1 control microtubule stability, plant growth, and drought response. *Plant Cell* 29: 169–191

Chinnusamy V, Ohta M, Kanrar S, Lee BH, Hong X, Agarwal M, Zhu JK (2003) ICE1: a regulator of cold-induced transcriptome and freezing tolerance in *Arabidopsis*. *Genes Dev* 17: 1043–1054

Clough SJ, Bent AF (1998) Floral dip: a simplified method for *Agrobacterium*-mediated transformation of *Arabidopsis thaliana*. *Plant J* 16: 735–743

Cybulski LE, Ballering J, Moussatova A, Inda ME, Vazquez DB, Wassenaar TA, de Mendoza D, Tieleman DP, Killian JA (2015) Activation of the bacterial thermosensor DesK involves a serine zipper dimerization motif that is modulated by bilayer thickness. *Proc Natl Acad Sci USA* 112: 6353–6358

Ding Y, Li H, Zhang X, Xie Q, Gong Z, Yang S (2015) OST1 kinase modulates freezing tolerance by enhancing ICE1 stability in *Arabidopsis*. *Dev Cell* 32: 278–289

Ding Y, Jia Y, Shi Y, Zhang X, Song C, Gong Z, Yang S (2018) OST1-mediated BTF3L phosphorylation positively regulates CBFs during plant cold responses. *EMBO J* 37: e98228

Doherty CJ, Van Buskirk HA, Myers SJ, Thomashow MF (2009) Roles for *Arabidopsis* CAMTA transcription factors in cold-regulated gene expression and freezing tolerance. *Plant Cell* 21: 972–984

Dong CH, Agarwal M, Zhang Y, Xie Q, Zhu JK (2006) The negative regulator of plant cold responses, HOS1, is a RING E3 ligase that mediates the ubiquitination and degradation of ICE1. *Proc Natl Acad Sci USA* 103: 8281–8286

Farazi TA, Waksman G, Gordon JI (2001) The biology and enzymology of protein N-myristoylation. *J Biol Chem* 276: 39501–39504

Fuchs S, Grill E, Meskiene I, Schweighofer A (2013) Type 2C protein phosphatases in plants. *FEBS J* 280: 681–693

Fujii H, Verslues PE, Zhu JK (2011) *Arabidopsis* decuple mutant reveals the importance of SnRK2 kinases in osmotic stress responses in vivo. *Proc Natl Acad Sci USA* 108: 1717–1722

Fujii H, Chinnusamy V, Rodrigues A, Rubio S, Antoni R, Park S-Y, Cutler SR, Sheen J, Rodriguez PL, Zhu J-K (2009) *In vitro* reconstitution of an abscisic acid signalling pathway. *Nature* 462: 660–664

Geiger D, Scherzer S, Mumm P, Stange A, Marten I, Bauer H, Ache P, Matschi S, Liese A, Al-Rasheid KA, Romeis T, Hedrich R (2009) Activity of guard cell anion channel SLAC1 is controlled by drought-stress signaling kinase-phosphatase pair. *Proc Natl Acad Sci USA* 106: 21425–21430

Goldberg J (1998) Structural basis for activation of ARF GTPase: mechanisms of guanine nucleotide exchange and GTP-myristoyl switching. *Cell* 95: 237–248

Guo XY, Liu DF, Chong K (2018) Cold signaling in plants: insights into mechanisms and regulation. *J Integr Plant Biol* 60: 745–756

Guy CL (1990) Cold acclimation and freezing stress tolerance: role of protein metabolism. *Annu Rev Plant Physiol Plant Mol Biol* 41: 187–223

Hannoush RN (2015) Synthetic protein lipidation. *Curr Opin Chem Biol* 28: 39–46

Hao Q, Yin P, Li W, Wang L, Yan C, Lin Z, Wu JZ, Wang J, Yan SF, Yan N (2011) The molecular basis of ABA-independent inhibition of PP2Cs by a subclass of PYL proteins. *Mol Cell* 42: 662–672

Ishitani M, Liu JP, Halfter U, Kim CS, Shi WM, Zhu JK (2000) SOS3 function in plant salt tolerance requires N-myristoylation and calcium binding. *Plant Cell* 12: 1667–1677

Jia YX, Ding YL, Shi YT, Zhang XY, Gong ZZ, Yang SH (2016) The *cbfs* triple mutants reveal the essential functions of CBFs in cold acclimation and allow the definition of CBF regulons in *Arabidopsis*. *New Phytol* 212: 345–353

Jiang BC, Shi YT, Zhang XY, Xin XY, Qi LJ, Guo HW, Li JG, Yang SH (2017) PIF3 is a negative regulator of the CBF pathway and freezing tolerance in *Arabidopsis*. *Proc Natl Acad Sci USA* 114: E6695–E6702

Lee CM, Thomashow MF (2012) Photoperiodic regulation of the C-repeat binding factor (*CBF*) cold acclimation pathway and freezing tolerance in *Arabidopsis thaliana*. *Proc Natl Acad Sci USA* 109: 15054–15059

Li H, Ding YL, Shi YT, Zhang XY, Zhang SQ, Gong ZZ, Yang SH (2017a) MPK3-and MPK6-mediated ICE1 phosphorylation negatively regulates ICE1 stability and freezing tolerance in *Arabidopsis*. *Dev Cell* 43: 630–642

Li H, Ye K, Shi Y, Cheng J, Zhang X, Yang S (2017b) BZR1 positively regulates freezing tolerance via CBF-dependent and CBF-independent pathways in *Arabidopsis*. *Mol Plant* 10: 545–559

Liu JY, Shi YT, Yang SH (2018) Insights into the regulation of C-repeat binding factors in plant cold signaling. *J Integr Plant Biol* 60: 780–795

Liu Q, Kasuga M, Sakuma Y, Abe H, Miura S, Yamaguchi-Shinozaki K, Shinozaki K (1998) Two transcription factors, DREB1 and DREB2, with an EREBP/AP2 DNA binding domain separate two cellular signal transduction pathways in drought- and low-temperature-responsive gene expression, respectively, in *Arabidopsis*. *Plant Cell* 10: 1391–1406

Liu Z, Jia Y, Ding Y, Shi Y, Li Z, Guo Y, Gong Z, Yang S (2017) Plasma membrane CRPK1-mediated phosphorylation of 14-3-3 proteins induces their nuclear import to fine-tune CBF signaling during cold response. *Mol Cell* 66: 117–128 e115

Ma Y, Szostkiewicz I, Korte A, Moes D, Yang Y, Christmann A, Grill E (2009) Regulators of PP2C phosphatase activity function as abscisic acid sensors. *Science* 324: 1064–1068

Ma Y, Dai X, Xu Y, Luo W, Zheng X, Zeng D, Pan Y, Lin X, Liu H, Zhang D, Chong K (2015) *COLD1* confers chilling tolerance in Rice. *Cell* 160: 1209–1221

Martinez L, Reeves A, Haldenwang W (2010) Stressosomes formed in *Bacillus subtilis* from the RsbR protein of listeria monocytogenes allow sigma(B) activation following exposure to either physical or nutritional stress. *J Bacteriol* 192: 6279–6286

Mclaughlin S, Aderem A (1995) The myristoyl-electrostatic switch - a modulator of reversible protein-membrane interactions. *Trends Biochem Sci* 20: 272–276

de Mendoza D (2014) Temperature sensing by membranes. *Annu Rev Microbiol* 68: 101–116

Miura K, Jin JB, Lee J, Yoo CY, Stirm V, Miura T, Ashworth EN, Bressan RA, Yun DJ, Hasegawa PM (2007) SIZ1-mediated sumoylation of ICE1 controls *CBF3/DREB1A* expression and freezing tolerance in *Arabidopsis*. *Plant Cell* 19: 1403–1414

Monaghan J, Matschi S, Shorinola O, Rovenich H, Matei A, Segonzac C, Malinovsky FG, Rathjen JP, MacLean D, Romeis T, Zipfel C (2014) The calcium-dependent protein kinase CPK28 buffers plant immunity and regulates BIK1 turnover. *Cell Host Microbe* 16: 605–615

Nakashima K, Yamaguchi-Shinozaki K (2013) ABA signaling in stress-response and seed development. *Plant Cell Rep* 32: 959–970

Ni M, Cui D, Einstein J, Narasimhulu S, Vergara CE, Gelvin SB (1995) Strength and tissue-specificity of chimeric promoters derived from the octopine and mannopine synthase genes. *Plant J* 7: 661–676

Park SY, Fung P, Nishimura N, Jensen DR, Fujii H, Zhao Y, Lumba S, Santiago J, Rodrigues A, Chow TF, Alfred SE, Bonetta D, Finkelstein R, Provart NJ, Desveaux D, Rodriguez PL, McCourt P, Zhu JK, Schroeder JI, Volkman BF *et al* (2009) Abscisic acid inhibits type 2C protein phosphatases via the PYR/PYL family of START proteins. *Science* 324: 1068–1071

Pierre M, Traverso JA, Boisson B, Domenichini S, Bouchez D, Giglione C, Meinnel T (2007) N-myristoylation regulates the SnRK1 pathway in *Arabidopsis*. *Plant Cell* 19: 2804–2821

Robert N, Merlot S, N'Guyen V, Boisson-Dernier A, Schroeder JI (2006) A hypermorphic mutation in the protein phosphatase 2C HAB1 strongly affects ABA signaling in *Arabidopsis*. *FEBS Lett* 580: 4691–4696

Sato A, Sato Y, Fukao Y, Fujiwara M, Umezawa T, Shinozaki K, Hibi T, Taniguchi M, Miyake H, Goto DB, Uozumi N (2009) Threonine at position 306 of the KAT1 potassium channel is essential for channel activity and is a target site for ABA-activated SnRK2/OST1/SnRK2.6 protein kinase. *Biochem J* 424: 439–448

Shi Y, Ding Y, Yang S (2018) Molecular regulation of CBF signaling in cold acclimation. *Trends Plant Sci* 23: 623–637

Shi Y, Tian S, Hou L, Huang X, Zhang X, Guo H, Yang S (2012) Ethylene signaling negatively regulates freezing tolerance by repressing expression of *CBF* and type-A *ARR* genes in *Arabidopsis*. *Plant Cell* 24: 2578–2595

Sirichandra C, Gu D, Hu HC, Davanture M, Lee S, Djaoui M, Valot B, Zivy M, Leung J, Merlot S, Kwak JM (2009) Phosphorylation of the *Arabidopsis* AtrbohF NADPH oxidase by OST1 protein kinase. *FEBS Lett* 583: 2982–2986

Stockinger EJ, Gilmour SJ, Thomashow MF (1997) *Arabidopsis thaliana CBF1* encodes an AP2 domain-containing transcriptional activator that binds to the C-repeat/DRE, a cis-acting DNA regulatory element that stimulates transcription in response to low temperature and water deficit. *Proc Natl Acad Sci USA* 94: 1035–1040

Tang HY, Han M (2017) Fatty acids regulate germline sex determination through ACS-4-dependent myristoylation. *Cell* 169: 457–469

Thomashow MF (1999) Plant cold acclimation: freezing tolerance genes and regulatory mechanisms. *Annu Rev Plant Physiol Plant Mol Biol* 50: 571–599

Vlad F, Rubio S, Rodrigues A, Sirichandra C, Belin C, Robert N, Leung J, Rodriguez PL, Lauriere C, Merlot S (2009) Protein phosphatases 2C regulate the activation of the Snf1-related kinase OST1 by abscisic acid in *Arabidopsis*. *Plant Cell* 21: 3170–3184

Wright MH, Heal WP, Mann DJ, Tate EW (2010) Protein myristoylation in health and disease. *J Chem Biol* 3: 19–35

Yang H, Shi Y, Liu J, Guo L, Zhang X, Yang S (2010) A mutant CHS3 protein with TIR-NB-LRR-LIM domains modulates growth, cell death and freezing tolerance in a temperature-dependent manner in *Arabidopsis*. *Plant J* 63: 283–296

Yin P, Fan H, Hao Q, Yuan XQ, Wu D, Pang YX, Yan CY, Li WQ, Wang JW, Yan N (2009) Structural insights into the mechanism of abscisic acid signaling by PYL proteins. *Nat Struct Mol Biol* 16: 1230–U1242

Zhang Z, Li J, Li F, Liu H, Yang W, Chong K, Xu Y (2017) OsMAPK3 phosphorylates OsbHLH002/OsICE1 and inhibits its ubiquitination to activate OsTPP1 and enhances rice chilling tolerance. *Dev Cell* 43: 731–743 e735

Zhao C, Wang P, Si T, Hsu CC, Wang L, Zayed O, Yu Z, Zhu Y, Dong J, Tao WA, Zhu JK (2017) MAP kinase cascades regulate the cold response by modulating ICE1 protein stability. *Dev Cell* 43: 618–629 e615